Curcumin Inhibits Tumor Growth and Angiogenesis in Ovarian Carcinoma by Targeting the Nuclear Factor-κB Pathway

Yvonne G. Lin,[1] Ajaikumar B. Kunnumakkara,[2] Asha Nair,[2] William M. Merritt,[1] Liz Y. Han,[1] Guillermo N. Armaiz-Pena,[1,4] Aparna A. Kamat,[1] Whitney A. Spannuth,[1] David M. Gershenson,[1] Susan K. Lutgendorf,[6] Bharat B. Aggarwal,[2,5] and Anil K. Sood[1,3]

Abstract

Purpose: Curcumin, a component of turmeric, has been shown to suppress inflammation and angiogenesis largely by inhibiting the transcription factor nuclear factor-κB (NF-κB). This study evaluates the effects of curcumin on ovarian cancer growth using an orthotopic murine model of ovarian cancer.

Experimental Design: *In vitro* and *in vivo* experiments of curcumin with and without docetaxel were done using human ovarian cancer cell lines SKOV3ip1, HeyA8, and HeyA8-MDR in athymic mice. NF-κB modulation was ascertained using electrophoretic mobility shift assay. Evaluation of angiogenic cytokines, cellular proliferation (proliferating cell nuclear antigen), angiogenesis (CD31), and apoptosis (terminal deoxynucleotidyl transferase–mediated dUTP nick end labeling) was done using immunohistochemical analyses.

Results: Curcumin inhibited inducible NF-κB activation and suppressed proliferation *in vitro*. *In vivo* dose-finding experiments revealed that 500 mg/kg orally was the optimal dose needed to suppress NF-κB and signal transducers and activators of transcription 3 activation and decrease angiogenic cytokine expression. In the SKOV3ip1 and HeyA8 *in vivo* models, curcumin alone resulted in 49% ($P = 0.08$) and 55% ($P = 0.01$) reductions in mean tumor growth compared with controls, whereas when combined with docetaxel elicited 96% ($P < 0.001$) and 77% reductions in mean tumor growth compared with controls. In mice with multidrug-resistant HeyA8-MDR tumors, treatment with curcumin alone and combined with docetaxel resulted in significant 47% and 58% reductions in tumor growth, respectively ($P = 0.05$). In SKOV3ip1 and HeyA8 tumors, curcumin alone and with docetaxel decreased both proliferation ($P < 0.001$) and microvessel density ($P < 0.001$) and increased tumor cell apoptosis ($P < 0.05$).

Conclusions: Based on significant efficacy in preclinical models, curcumin-based therapies may be attractive in patients with ovarian carcinoma.

Author's Affiliations: [1]Department of Gynecologic Oncology, [2]Cytokine Research Laboratory, Department of Experimental Therapeutics, and [3]Department of Cancer Biology, The University of Texas M. D. Anderson Cancer Center; [4]Program in Cancer Biology and [5]Program in Immunology, University of Texas Graduate School of Biomedical Sciences at Houston, Houston, Texas; and [6]Department of Psychology, University of Iowa, Iowa City, Iowa

Received 12/26/06; revised 2/26/07; accepted 3/14/07.

Grant support: National Cancer Institute/Department of Health and Human Services/NIH Training of Academic Gynecologic Oncologists grant T32-CA101642 (Y.G. Lin, W.M. Merritt, and W.A. Spannuth), Marcus Foundation, NIH grants CA 10929801 and 11079301, The University of Texas M. D. Anderson Specialized Program of Research Excellence in ovarian cancer grant P50CA083639 (A.K. Sood), Clayton Foundation for Research, NIH PO1 grant CA91844 on lung chemoprevention, and NIH P50 Head and Neck Specialized Program of Research Excellence grant P50CA97007 (B.B. Aggarwal).

The costs of publication of this article were defrayed in part by the payment of page charges. This article must therefore be hereby marked *advertisement* in accordance with 18 U.S.C. Section 1734 solely to indicate this fact.

Requests for reprints: Anil K. Sood, Ovarian Cancer Research, Department of Gynecologic Oncology, The University of Texas M. D. Anderson Cancer Center, 1155 Herman Pressler, Unit 1352, Houston, TX 77030. Phone: 713-745-5266; Fax: 713-792-7586; E-mail: asood@mdanderson.org.

doi:10.1158/1078-0432.CCR-06-3072

Projected to be responsible for more than 15,000 deaths in 2006, ovarian cancer remains the leading cause of death from gynecologic cancer (1). The current standard of care includes primary surgical cytoreduction followed by cytotoxic chemotherapy; however, recurrence remains a significant problem. Therefore, the need for effective therapeutic strategies and targets while minimizing untoward side effects is paramount.

Turmeric (*Curcuma longa*) derived from the rhizome has been described as an anti-inflammatory agent. The active component of turmeric, curcumin (diferuloylmethane), has been shown to have antiviral, antibacterial, antioxidant, anti-inflammatory, antiproliferative, and antiangiogenic activities (2–4). Curcumin has also been shown to inhibit Akt activation and down-regulate the expression of cyclooxygenase-2 (COX-2), 5-lipooxygenase, vascular endothelial growth factor (VEGF), phosphorylated signal transducers and activators of transcription 3 (STAT3), and matrix metalloproteinase-9 (MMP-9), all of which are closely linked with tumorigenesis (5, 6). Both animal and human studies have suggested that curcumin may have potential in the treatment of inflammation and cancer (7–10). *In vitro* and *in vivo* preclinical studies have implicated curcumin

as an important mediator of cyclins and cell cycle arrest (11), apoptosis (12), cell adhesion (11), and angiogenesis (13).

Central to the wide range of effects curcumin exerts is its down-regulation of the transcription factor nuclear factor-κB (NF-κB). Our laboratory and others have shown that curcumin is a potent blocker of NF-κB activation, which has been linked with proliferation, invasion, and angiogenesis as well as suppression of apoptosis (14). Furthermore, NF-κB seems to play a key role in regulating the expression of multiple tumorigenic and proangiogenic growth factors, such as interleukin-8 (IL-8), VEGF, COX-2 (15–18), as well as decreased apoptosis (12, 19). Some tumors, such as certain gastrointestinal carcinomas, seem to have constitutively active NF-κB, which is also associated with diminished overall survival rates (11). Targeting the NF-κB pathway seems to have therapeutic relevance in ovarian and other cancers. For example, blockade of NF-κB activation and its downstream antitumor and antiangiogenic activity using a synthetic proteasome inhibitor has shown some efficacy in diminishing ovarian tumor growth (20). However, the specific effects of this transcription factor in ovarian cancer pathogenesis are not fully understood.

Based on the ability of curcumin to block NF-κB activation and the possible role of NF-κB activation in ovarian carcinoma, we examined its effects on ovarian cancer growth in preclinical models using both chemotherapy-sensitive and chemotherapy-resistant cell lines.

Materials and Methods

Cell lines. These studies used three highly metastatic human ovarian cancer cell lines: SKOV3ip1, HeyA8, and the multidrug-resistant cell line HeyA8-MDR. The derivation and source of the cell lines have been reported elsewhere (21–23). SKOV3ip1 and HeyA8 cells were grown at 37°C as monolayer cultures in RPMI 1640 supplemented with 15% fetal bovine serum and 0.1% gentamicin sulfate (Gemini Bio-Products). The HeyA8-MDR cell line was made available as a generous gift from Dr. Isaiah J. Fidler (The University of Texas M. D. Anderson Cancer Center, Houston, TX) and generated through sequential exposure to increasing sublethal concentrations of paclitaxel. HeyA8-MDR cells were grown in the same medium as the parental cells supplemented with 300 μg/mL paclitaxel (Bristol-Myers Squibb Co.). All tumor cell lines were regularly screened for Mycoplasma using MycoAlert (Cambrex Bioscience) as described by the manufacturer. *In vitro* and *in vivo* experiments were conducted with cell lines at 70% to 80% confluence.

Curcumin. Curcumin (>98% pure) was obtained from Sabinsa Corp. *In vivo* studies were conducted using curcumin homogenized in Super Refined Sesame Oil NF-NP (Croda, Inc.) into a concentration of 10 mg/100 μL. To control and standardize the amount of drug delivered, curcumin was given by oral gavage to each mouse daily.

Cytotoxicity assay. The cytotoxic effects of tumor necrosis factor-α (TNF-α) and curcumin were determined by the 3-(4,5-dimethylthiazol-2-yl)-2,5-diphenyltetrazolium bromide uptake method as described previously (24). Briefly, 2,000 SKOV3ip1 and HeyA8 cells were incubated with RPMI 1640 supplemented with 10% fetal bovine serum in triplicate in a 96-well plate and then treated with the indicated concentrations of TNF-α or curcumin at 37°C for 24 h. A 3-(4,5-dimethylthiazol-2-yl)-2,5-diphenyltetrazolium bromide solution was added to each well and incubated at 37°C for 2 h. An extraction buffer (20% SDS, 50% dimethylformamide) was added, and the cells were incubated at 37°C overnight. The absorbance was measured at 570 nm using a 96-well multiscanner (MRX Revelation, Dynex Technologies).

LIVE/DEAD assay. Apoptosis was measured using the LIVE/DEAD Viability/Cytotoxicity kit (Molecular Probes, Invitrogen Corp.) that determines the intracellular esterase activity and plasma membrane integrity of cells by using the green fluorescent polyanionic dye calcein, which is retained within live cells in conjunction with the red fluorescent monomeric dye ethidium, which is excluded by the intact plasma membrane of live cells, but can enter apoptotic cells through damaged membranes to bind to nucleic acids. This assay was done as described previously (25). Briefly, after allowing the cells to adhere, 5,000 HeyA8 or SKOV3ip1 cells/chamber slide were coincubated with and without curcumin (10 μmol/L) and docetaxel (10, 25, and 50 nmol/L) at 37°C for 24 h. Cells were stained with the LIVE/DEAD assay reagent (5 μmol/L ethidium homodimer and 5 μmol/L calcein-AM) and then incubated at 37°C for 30 min. Cells were then analyzed by fluorescent microscopy (Labophot 2, Nikon). The number of live (green) and dead (red) cells was counted to generate the percentage of dead cells.

Electrophoretic mobility shift assays. To determine the effect of curcumin on NF-κB activation after stimulation with TNF-α, 10^6 SKOV3ip1 cells were treated with 10 μmol/L curcumin for 3, 6, 12, 48, and 72 h and then exposed to TNF-α (0.1 nmol/L) for 30 min. To determine NF-κB activation, we prepared nuclear extracts and did electrophoretic mobility shift assays (EMSA) as described previously (26). For supershift assays, nuclear extracts prepared from TNF-treated cells were incubated with antibodies against either the p50 or the p65 subunit of NF-κB at 37°C for 15 min before the complex was analyzed by EMSA. Preimmune serum was included as the negative control. The dried gels were visualized, and the radioactive bands were quantitated with a Storm 820 and ImageQuant software (Amersham).

Immunohistochemistry. For NF-κB, COX-2, and phosphorylated STAT3 immunohistochemistry, the DakoCytomation kit (Dako) was used. Briefly, formalin-fixed, paraffin-embedded slides were deparaffinized with acetone followed by descending grades of ethanol. Slides were then incubated in p65, COX-2, and phosphorylated STAT3 antibodies (1:100 dilution; Santa Cruz Biotechnology, Inc.) at 4°C overnight. Slides were then developed with streptavidin-biotin (Dako) and visualized with 3,3′-diaminobenzidine (Open Biosystems). Pictures were captured using a Photometrics CoolSNAP CF color camera (Nikon) and MetaMorph version 4.6.5 software (Universal Imaging).

For detecting VEGF, MMP-9, IL-8, and proliferating cell nuclear antigen (PCNA) immunoreactivity, formalin-fixed, paraffin-embedded serial sections were deparaffinized by sequential washing of xylene followed by descending grades of ethanol. Depending on the antibody used, antigen retrieval was achieved by either citrate buffer (pH 6.0) in a steamer (MMP-9, IL-8, and PCNA) or pepsin in a 37°C humidified incubator (VEGF). Endogenous peroxidases were blocked with 3% H_2O_2 in PBS (IL-8) or methanol (VEGF and MMP-9). Nonspecific proteins and exposed epitopes were blocked with 5% normal horse serum/1% normal goat serum, and slides were incubated at 4°C overnight with the respective primary antibody at the following dilutions: 1:100 VEGF (Santa Cruz Biotechnology), 1:400 MMP-9 (Chemicon-Millipore), 1:25 IL-8 (BioSource International, Inc.), and 1:50 PCNA (Dako). After PBS washes, the appropriate secondary antibody was applied for 1 h at room temperature. Visualization was achieved with 3,3′-diaminobenzidine chromagen. All counterstaining was done with Gill's hematoxylin (Sigma-Aldrich). Proliferative index was calculated by the percentage of PCNA-positive cells over five randomly selected high-power fields.

To quantify angiogenesis, microvessel density (MVD) was ascertained by counting CD31-positive vessels as described previously (27, 28). In brief, 8-μm sections were fixed and incubated with anti-mouse CD31 (1:800; PharMingen) at 4°C overnight. MVD was calculated by taking five representative photographs (×100 magnification) of each slide and counting the number of vessels per field. A vessel was defined as an open lumen with at least one CD31-positive cell immediately adjacent to it.

To quantify apoptosis, terminal deoxynucleotidyl transferase (TdT)-mediated dUTP nick end labeling assay was done on 5-μm-thick paraffin-embedded tumor slides as described previously (27). Briefly,

after deparaffinization, all slides were treated with proteinase K (1:500) with one slide treated with DNase as a positive control. Endogenous peroxidases were blocked with 3% H_2O_2 in methanol. After rinsing with TdT buffer (30 mmol/L Trizma, 140 mmol/L sodium cacodylate, 1 mmol/L cobalt chloride), slides were incubated with terminal transferase (1:400; Roche Diagnostics) and biotin-16-dUTP (1:200; Roche Diagnostics) in TdT buffer and then blocked with 2% bovine serum albumin. Samples were then incubated in peroxidase streptavidin (1:400), visualized with 3,3′-diaminobenzidine chromagen, and counterstained with Gill's hematoxylin. Apoptotic index was determined by the number of apoptotic tumor cells in five randomly selected high-power fields exclusive of necrotic areas.

Animals. Female athymic nude mice (NCr-*nu*) were purchased from the National Cancer Institute-Frederick Cancer Research and Development Center. The mice were housed and maintained under specific pathogen-free conditions in accordance with guidelines from the American Association for Accreditation of Laboratory Animal Care and the NIH. All studies were approved and overseen by The University of Texas M. D. Anderson Cancer Center Institutional Animal Care and Use Committee.

Orthotopic implantation of tumor cells and necropsy procedures. At 70% to 80% confluence, SKOV3ip1, HeyA8, and HeyA8-MDR cells were collected from cultures using either 0.25% trypsin-EDTA (Life Technologies) or 0.1% EDTA depending on the cell line. Cells lifted with trypsin were neutralized with medium containing fetal bovine serum, centrifuged, and then resuspended in serum-free HBSS (Invitrogen). Cell lines not requiring trypsin neutralization were directly centrifuged at 1,000 rpm for 7 min at 4°C, washed with PBS, and then resuspended in serum-free HBSS. SKOV3ip1 and HeyA8-MDR cells were injected i.p. at a concentration of 1×10^6/200 μL HBSS. HeyA8 cells were injected i.p. at a concentration of 2.5×10^5/200 μL HBSS.

Therapy experiments were done using all three cell lines. Mice were sacrificed when the control group seemed near moribund, approximately 3 to 5 weeks after commencing therapy, depending on the cell line. Tumors were harvested from the peritoneal cavities of mice and weighed. Malignant ascites was aspirated and the volume was measured. For immunohistochemistry requiring frozen tissue, tumors were embedded in OCT (Miles, Inc.) at the time of tumor collection, snap frozen in liquid nitrogen, and stored at -80°C. Additional tissue for immunohistochemistry was formalin fixed at the time of tumor collection and then paraffin embedded.

Therapy experiments using curcumin in orthotopic murine models. Dose-finding experiments were done by injecting HeyA8 tumor cells i.p. (2.5×10^5) into athymic female mice. Nineteen days after tumor cell injection, the mice were randomized into five groups (20 mice per group): 0 mg, 100 mg/kg, 500 mg/kg, 1 g/kg, and 2 g/kg. Once daily curcumin or vehicle was given by oral gavage daily for 2 days. Mice were sacrificed at 6, 24, 48, and 72 h and 6 days after the last oral dose. Immunohistochemistry and EMSA were done on the tumors as described earlier.

To determine the antitumor effects of curcumin, we initiated treatment with daily curcumin gavage 1 week after the injection of tumor cells using a minimal residual disease model (27–31). Docetaxel (35 μg for SKOV3ip1 or 50 μg for HeyA8 and HeyA8-MDR; Sanofi-Aventis) or vehicle was injected i.p. once weekly (27). Docetaxel was the chosen taxane given its favorable side effect profile over paclitaxel in human studies (32–34). Curcumin (500 mg/kg) or vehicle was given by gavage once daily. Mice were monitored daily for adverse effects, and tumors were harvested at necropsy ~4 weeks after initiation of therapy or when any of the control mice began to seem moribund. Mouse weight, tumor weight, tumor distribution, and ascites volume were recorded.

Statistical analysis. The Mann-Whitney rank sum test was used to analyze nonparametric, nonnormally distributed data sets. Statistical analyses were done using Statistical Package for the Social Sciences 12.0 for Windows (SPSS, Inc.). A two-tailed P value of ≤ 0.05 was deemed statistically significant.

Results

In vitro *effects of curcumin on ovarian carcinoma.* Before *in vivo* experiments, we examined the *in vitro* effects of curcumin on ovarian carcinoma cytotoxicity. We first determined by 3-(4,5-dimethylthiazol-2-yl)-2,5-diphenyltetrazolium bromide assay that the IC_{50} level for both the HeyA8 and SKOV3ip1 cell lines was 10 μmol/L (Fig. 1A). Curcumin was also found to confer additional benefit in HeyA8 and SKOV3ip1 cellular apoptosis beyond that provided by docetaxel (Fig. 1B). Treatment of HeyA8 with varying doses of docetaxel alone resulted in ~50% cell death at ~35 nmol/L; however, the addition of curcumin at the IC_{50} dose of 10 μmol/L resulted in a 5-fold decrease of docetaxel needed to achieve the equivalent amount of cell death. This enhanced effect was similarly remarkable in the SKOV3ip1 cell line where a docetaxel dose of 50 nmol/L was needed to achieve ~50% cell death compared with <10 nmol/L docetaxel when it was given with curcumin at the IC_{50} dose.

Based on the role of curcumin in NF-κB inhibition, we did EMSA to determine the effects of curcumin on NF-κB activity in two ovarian cancer cell lines. NF-κB activation was induced by exposure to TNF-α in both the HeyA8 and the SKOV3ip1 cell lines; however, a brief 3-h exposure of 50 μmol/L curcumin abrogated this effect (data not shown). To determine whether using a lower dose of curcumin could elicit the same effects, cells were treated with the IC_{50} dose of 10 μmol/L curcumin for various times, both with and without TNF-α induction. The lower curcumin dose was also found to be efficacious in inhibiting NF-κB activation within 6 h of treatment (Fig. 1C).

In vivo *effects of curcumin on ovarian carcinoma.* For *in vivo* work, we first conducted dose-finding experiments to determine the optimal curcumin dose and frequency for down-regulating angiogenic factors. Two once daily doses of curcumin at 0 mg/kg, 100 mg/kg, 500 mg/kg, 1 g/kg, or 2 g/kg were given by gavage to athymic female mice (n = 5 per group) bearing HeyA8 i.p. tumors 19 days after tumor cell injection. Animals were sacrificed 24 h, 48 h, 72 h, or 6 days after the last dose. Tumors collected from the mice were examined by immunohistochemistry and EMSA to determine duration of action of curcumin. Curcumin doses of ≥500 mg/kg consistently blocked NF-κB activation through 48 h (data not shown) compared with controls. Although NF-κB activity on EMSA began to return at 72 h, the degree of activity was still decreased relative to controls (data not shown). Similarly, using immunohistochemistry, we observed maximal NF-κB and phosphorylated STAT3 suppression by curcumin at 24 h after last exposure (Fig. 2A). By 72 h, expression levels of these factors had essentially returned to baseline. The decrease in VEGF, IL-8, and MMP-9 expression in response to curcumin exposure began as early as 6 h after the last dose and in some cases persisted up to 72 h from the last dose (Fig. 2B). Maximal inhibition of COX-2 was also observed 24 h after the last exposure to curcumin (Fig. 2C). Because clear down-regulation of transcription and angiogenic factors was most consistently observed and sustained at 24 h after treatment using the 500 mg/kg dose, subsequent *in vivo* therapy experiments used curcumin dosed at 500 mg/kg every 24 h.

To determine the antitumor effects of curcumin, multiple *in vivo* experiments were conducted. Curcumin therapy was initiated 1 week after tumor cell inoculation to model the

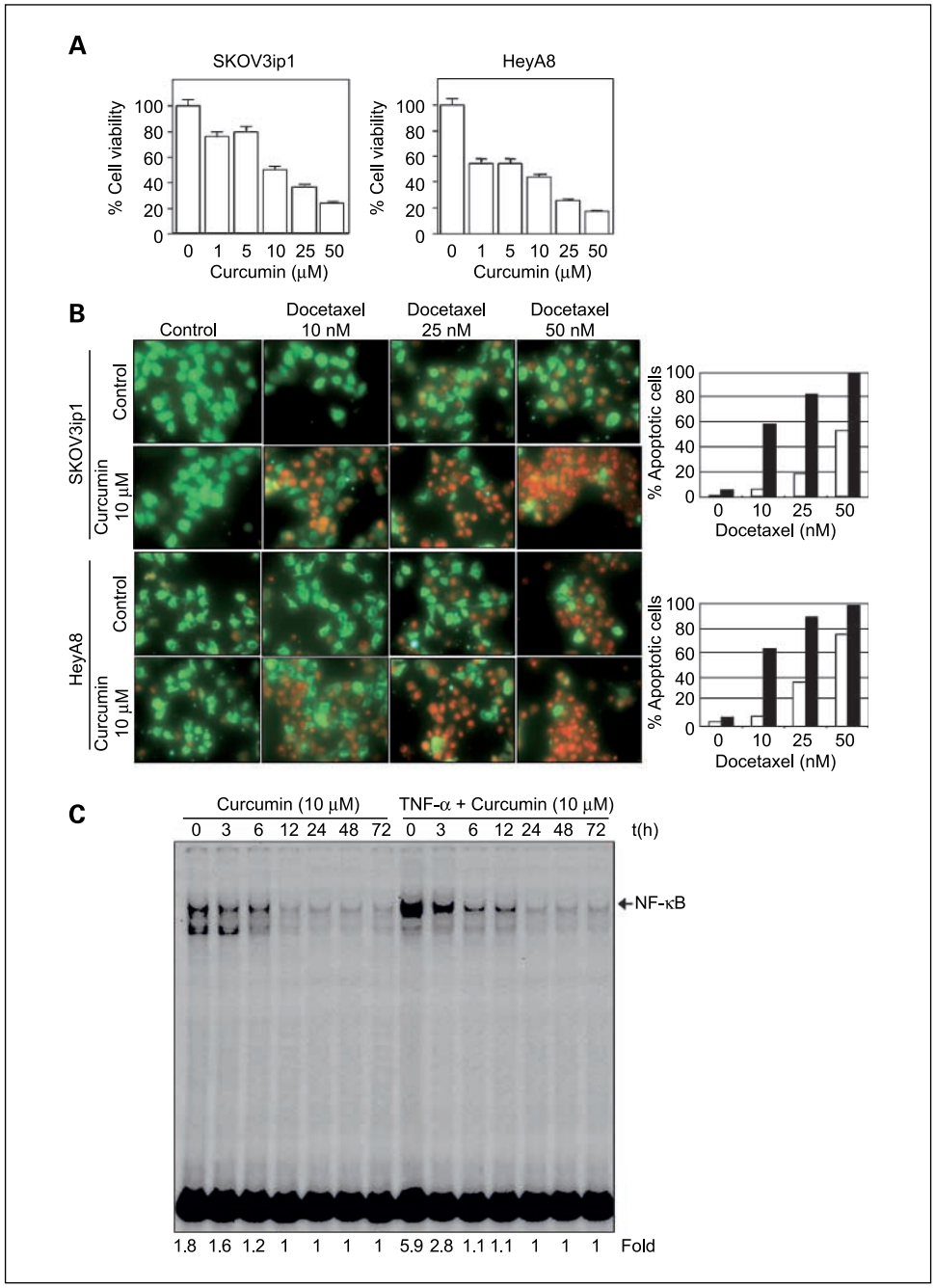

Fig. 1. *A,* cytotoxicity [3-(4,5-dimethylthiazol-2-yl)-2,5-diphenyltetrazolium bromide] graphs depicting the inhibitory concentration at 50% for SKOV3ip1 and HeyA8 cell lines *in vitro*. Varying doses of curcumin were given to HeyA8 and SKOV3ip1 cells (2,000 in 0.1 mL) for 72 h. Cell viability was analyzed by 3-(4,5-dimethylthiazol-2-yl)-2,5-diphenyltetrazolium bromide method. *B,* apoptosis induction by docetaxel with (*black columns*) and without (*white columns*) curcumin in SKOV3ip1 and HeyA8 cells. Cells were coincubated with medium or the IC_{50} dose of curcumin (10 μmol/L) and varying doses of docetaxel. *C,* EMSA shows curcumin-mediated inhibition of TNF-α–induced (0.1 nmol/L for 30 min) NF-κB activation. Cells were treated with 10 μmol/L curcumin for 3, 6, 12, 24, 48, and 72 h.

clinical scenario of minimal residual disease. The four treatment groups consisted of (*a*) vehicle alone, (*b*) docetaxel i.p. once weekly, (*c*) curcumin daily, and (*d*) curcumin daily with docetaxel weekly. Curcumin monotherapy resulted in a near significant 49% decrease in tumor weight ($P = 0.08$) in the SKOV3ip1 model and a 55% decrease in the HeyA8 model ($P = 0.01$; Fig. 3A and B). As expected, docetaxel was also effective in reducing tumor growth. The combination of curcumin and docetaxel had the greatest efficacy with 96% reduction in tumor burden in SKOV3ip1 ($P < 0.001$) and a 77% reduction in HeyA8 tumors ($P = 0.002$) compared with controls. Furthermore, combination of curcumin and docetaxel showed significant efficacy above docetaxel in the SKOV3ip1 model by reducing tumor mass by 66% beyond docetaxel monotherapy ($P = 0.01$).

Because advanced ovarian cancer often becomes refractory to traditional cytotoxic agents, we also examined the effects of curcumin in the multidrug-resistant HeyA8-MDR model. As expected, docetaxel monotherapy did not affect tumor growth compared with controls. Curcumin monotherapy exhibited a significant 47% reduction in tumor burden compared with controls ($P = 0.05$; Fig. 3C). Although no statistically significant difference was detected between curcumin monotherapy and combination therapy groups ($P = 0.3$), mice treated with curcumin and docetaxel showed a significant 58% reduction in tumor burden compared with controls ($P = 0.01$).

In addition to tumor weight, we also examined the effects of curcumin on tumor nodule formation (Table 1). Curcumin treatment both alone and in combination with docetaxel in the SKOV3ip1 tumors resulted in significantly reduced tumor nodule formation compared with controls ($P = 0.048$ and $P < 0.001$, respectively). Combination therapy resulted in a significant decrease in the median number of tumor nodules compared with docetaxel alone ($P = 0.04$). In both the HeyA8 and the HeyA8-MDR models, curcumin combined with docetaxel resulted in 63% and 25% reductions, respectively, in the median number of tumor nodules compared with controls ($P = 0.06$ for both comparisons). Daily monitoring of the animals throughout the course of therapy showed acceptable tolerability with no untoward side effects, such as changes in body weight, mobility, posture, feeding habits, and bowel habits.

Effects of curcumin on proliferation, MVD, and apoptosis. To determine possible mechanisms underlying curcumin-mediated suppression of tumor growth, we first examined its effects on tumor cell proliferation by doing PCNA immunohistochemistry

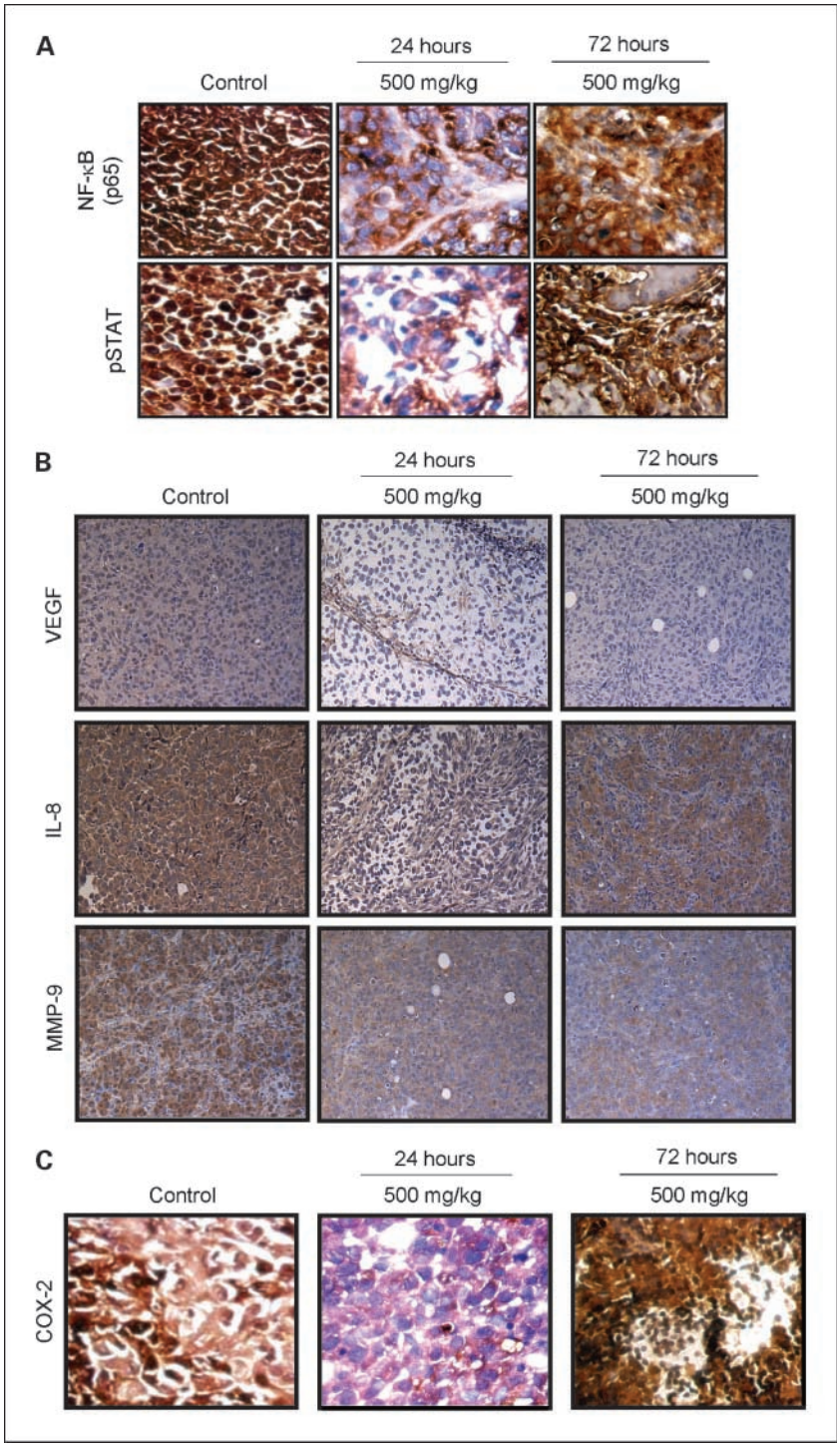

Fig. 2. *A,* effect of curcumin on transcription factors NF-κB and activated STAT3 as examined by immunohistochemistry. Magnification, ×200. Maximal down-regulation of these transcription factors is seen by 24 h after exposure to curcumin (500 mg/kg). Expression of NF-κB and STAT3 is back to baseline by 72 h after exposure. *B,* effect of curcumin on VEGF, IL-8, and MMP-9 as examined by immunohistochemistry. Magnification, ×100. *C,* effect of curcumin on COX-2 as seen on immunohistochemistry. Magnification, ×200.

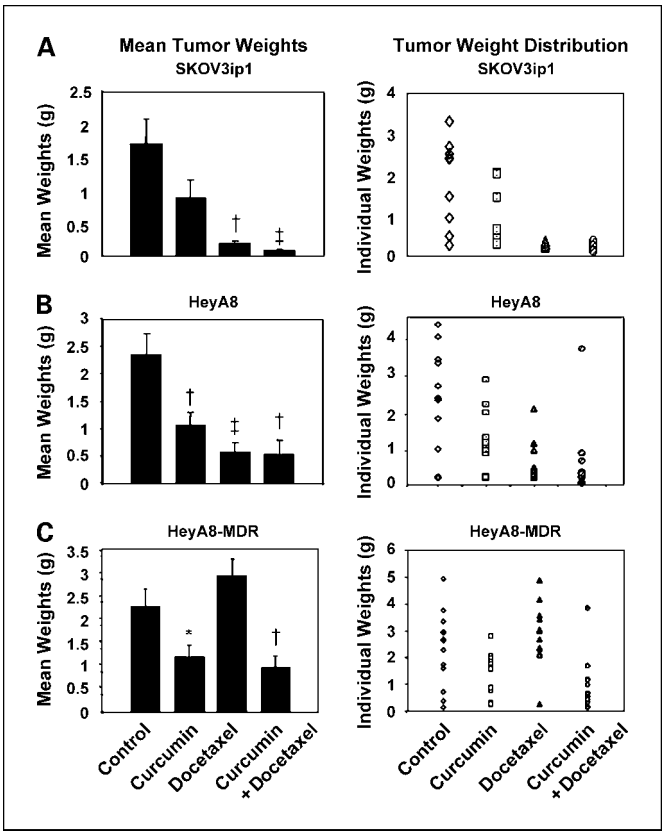

Fig. 3. Mean tumor weights and distribution from curcumin therapy experiments. Mice inoculated with SKOV3ip1 (*A*), HeyA8 (*B*), and HeyA8-MDR (*C*) received either vehicle alone (control), curcumin alone (500 mg/kg), docetaxel alone (35 or 50 μg once weekly depending on cell line), or combination curcumin plus docetaxel. Animals from all groups were sacrificed when control animals were moribund (approximately 3-4 weeks after initiating therapy depending on the cell line used). All tumors were harvested; the tumor weight and number of nodules were recorded. Columns, mean tumor weights for each sample group; bars, SE. *, $P \leq 0.05$; †, $P \leq 0.01$; ‡, $P \leq 0.001$.

on tumors obtained at necropsy from the therapy experiments. In the SKOV3ip1 model, the proliferation index for the control group was 80%; however, treatment with curcumin resulted in significantly lower proliferation indices across all treatment groups (18% reduction with curcumin alone, 21% with docetaxel alone, all *P*s < 0.001; Fig. 4A). Combination therapy with curcumin and docetaxel also resulted in a statistically significant 28% decrease in proliferation compared with docetaxel alone ($P = 0.008$). Similarly, significant decreases in proliferation were noted in response to curcumin-based monotherapy and combination therapy in the HeyA8 model ($P < 0.001$; data not shown).

Based on the observed decreases in angiogenic factors by immunohistochemistry, we sought to determine whether tumor angiogenesis was affected in our models. MVD, calculated as a measure of angiogenesis, was significantly lower with curcumin as monotherapy and as combination therapy in the SKOV3ip1 model ($P < 0.001$ and $P = 0.01$, respectively; Fig. 4B). Treatment with docetaxel did not result in a decrease in MVD compared with controls ($P = 0.07$). In tumors from the HeyA8 cell line, treatment with curcumin plus docetaxel resulted in a 30% decrease in MVD compared with controls ($P = 0.002$). The reduction in MVD due to combination therapy with curcumin and docetaxel was also significantly lower than the docetaxel alone group ($P < 0.001$).

To further elucidate the mechanism by which curcumin elicits its antitumor effects, we examined tumor cell apoptosis using the TdT-mediated dUTP nick end labeling assay in animals bearing SKOV3ip1 tumors. Treatment with curcumin resulted in a significant increase in apoptotic cells ($P = 0.04$; data not shown) compared with controls. There was also a significant increase in apoptotic cells in the combination curcumin/docetaxel group ($P = 0.01$) compared with vehicle-treated animals.

Discussion

The key findings from the current study are that curcumin has efficacy in ovarian carcinoma models via antitumorigenic and antiangiogenic mechanisms. Curcumin-based therapy had efficacy in both chemotherapy-sensitive and chemotherapy-resistant ovarian cancer models. Furthermore, we show that these effects are likely mediated through the NF-κB pathway as well as other transcription and angiogenic growth factors, including phosphorylated STAT3, COX-2, IL-8, MMP-9, and VEGF.

In vitro studies support the important role NF-κB plays in tumor growth (10, 15, 17, 35), apoptosis (12, 36), and tumor chemoresistance (11). Shi et al. (37) recently used Western blot analysis to show an increase in the apoptosis marker Bax and decreased cell survival factors, such as Bcl-2 and Bcl-X_L, after ovarian cancer cells were treated with curcumin; however, the direct effects of altering these factors by functional studies of apoptosis, such as TdT-mediated dUTP nick end labeling, were not elucidated. Curcumin also has demonstrable *in vitro* activity against NF-κB activation in many models (38). For example, some tumor cells have been reported to have constitutively activated NF-κB, which could be inhibited by curcumin (39). The inhibitory effects of curcumin on NF-κB activation are thought to be due to inhibition of IκB kinase activity, thereby essentially preventing NF-κB from successfully translocating into the nucleus to exert its downstream transcription events (39, 40). Our *in vitro* studies confirm the potent inhibitory effect of curcumin on TNF-α–induced NF-κB activation and suppression of key downstream tumorigenic and angiogenic factors important for tumor metastasis. These results indicate that curcumin exerts both direct and indirect (via angiogenic mechanisms) antitumor effects. We extended our *in vitro* findings to *in vivo* experiments directly examining tumor cell apoptosis by TdT-mediated dUTP nick end labeling staining on formed tumor specimens. We showed that curcumin treatment indeed increased the number of TdT-mediated dUTP nick end labeling–positive cells within orthotopically implanted tumors in athymic mice.

To date, limited data exist about the effects of curcumin *in vivo*. Aggarwal et al. (8) reported suppression of paclitaxel-induced NF-κB activation in a breast cancer model. The authors also used immunohistochemical analyses to show that animals that were fed powdered curcumin via feed supplementation had diminished COX-2 and MMP-9 expression in breast cancer metastases in the lungs (8). However, because the curcumin powder was mixed into the feed at a 2% (w/w) composition, the true amount delivered into each mouse was not known. In a head and neck squamous cell carcinoma preclinical model,

Table 1. Effect of curcumin-based therapy on ovarian cancer growth

Cell line	Treatment	Median no. nodules (range)	*P* (vs control)
SKOV3ip1	Control	24 (2-32)	
	Curcumin	4.5 (1-26)	0.048
	Docetaxel	3 (2-5)	0.01
	Curcumin + docetaxel	1.5 (1-5)	<0.001
HeyA8	Control	4 (1-6)	
	Curcumin	3 (1-12)	NS
	Docetaxel	1.5 (1-5)	0.01
	Curcumin + docetaxel	1.5 (1-15)	0.06
HeyA8-MDR	Control	4 (1-11)	
	Curcumin	3 (1-11)	NS
	Docetaxel	9 (2-17)	0.02
	Curcumin + docetaxel	3 (1-10)	0.06

Abbreviation: NS, not significant.

LoTempio et al. (10) were unable to show antitumor effects using intratumoral curcumin/DMSO injections; however, they were able to achieve tumor inhibition using a topical curcumin paste applied once daily in nude mice bearing CAL27 tumors. Again, the true amount of curcumin absorbed via this route using a saline-based paste is not known and could not be quantified. To control for the dosing variability among animals, we delivered curcumin by oral gavage. Furthermore, we did dose-finding experiments in which each animal received the same carefully controlled optimal biological oral dose of curcumin.

The potential therapeutic role of curcumin in conjunction with other therapeutic agents has been explored in an *in vitro* setting. Using curcumin in conjunction with the COX-2 inhibitor celecoxib, Lev-Ari et al. (41) showed that whereas either agent alone resulted in moderate inhibition of cell growth, when used together, a robust synergistic effect on cell growth inhibition was observed *in vitro*. Similar findings were also observed in a colorectal adenocarcinoma cell line (42). Our *in vitro* experiments showed that simultaneous treatment of cells with curcumin and taxane-based therapy resulted in a striking increase in tumor cell apoptosis. Our *in vivo* experiments showed augmented antitumor activity when curcumin was given with the cytotoxic chemotherapy agent docetaxel. Interestingly, the magnitude of this effect from combination therapy was above that elicited by docetaxel therapy alone, thus suggesting that combining these two agents may actually be a superior therapeutic choice. Furthermore, even in a chemorefractory model, we showed antitumor activity by administering curcumin alone and in combination with docetaxel.

In the clinical setting, most patients with ovarian cancer will develop recurrent chemoresistant tumors (1). Based on the role of NF-κB in cell proliferation, bypassing apoptosis, and promoting tumorigenesis (8, 20), it is an attractive clinical therapeutic target. A phase I trial using carboplatin in conjunction with the small-molecule inhibitor bortezomib, which blocks NF-κB activation by inhibiting the proteasome, reported a 47% overall response rate with two complete responses in patients with recurrent ovarian or primary peritoneal cancer (20). Although NF-κB activation was successfully inhibited, dose-limiting toxicities, including diarrhea, rash, neuropathy, and constipation, were observed (20). Our current study exploited the ability of curcumin to target and block NF-κB activation to produce the downstream inhibitory effects on angiogenesis and tumor growth. We showed that curcumin delivered by oral gavage successfully inhibited NF-κB activation and inhibited tumor growth and angiogenesis in our ovarian carcinoma models.

Although curcumin is considered a natural product, safety and toxicity questions nevertheless must be addressed. Several preclinical studies, including this current study, have shown no curcumin-related weight loss or adverse events in animals (8, 10). In limited human trials studying postoperative inflammation and rheumatoid arthritis, no adverse effects were reported in oral doses up to 2.1 g of curcumin daily (43, 44). In a chemopreventive trial, high doses of 12 g curcumin were intolerable for patients due to the sheer volume of tablets needed to achieve this dose; nevertheless, no adverse curcumin-related effects were reported in this early phase I trial (45). A recent dose escalation study in health volunteers showed minimal grade 1 adverse events (e.g., yellow stool, diarrhea, rash, and headache) that did not seem to be dose related (46). Additional studies are currently under way investigating compounds that may enhance the bioavailability and potency of curcumin (47). Furthermore, despite preliminary pharmacokinetic studies that suggest doses of up to 10 g

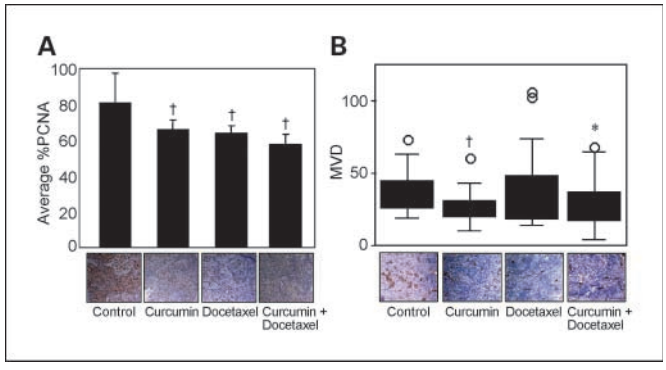

Fig. 4. *A,* proliferative index for SKOV3ip1 tumors with representative PCNA immunohistochemical sections from tumors collected at necropsy. *B,* box plot of MVD for SKOV3ip1 tumors with representative CD31 immunohistochemical sections from tumors collected at necropsy. ○, outliers. *, $P \leq 0.01$; †, $P \leq 0.001$.

daily are well tolerated among colon cancer patients (46, 48), well-designed pharmacokinetic studies should, nonetheless, be conducted before initiating therapeutic trials in patients with ovarian cancer to optimize dosage and dosing frequency.

In conclusion, our findings support the use of curcumin, alone and in combination with traditional cytotoxic agents, as an antitumorigenic and antiangiogenic therapy in ovarian cancer. Furthermore, the favorable safety profile of curcumin supports additional investigation into its use as a chemotherapeutic or a chemopreventive agent.

Acknowledgments

We thank Nicholas Jennings, Donna Reynolds, and Drs. Tae Jin Kim, Robert Langley, Gautam Sethi, Shishir Shishodia, and Yun-Fang Wang for their insightful discussions and expertise.

References

1. Overview: Ovarian cancer: how many women get ovarian cancer? 2006 [cited 2006 Feb 9]. Available from: http://www.cancer.org/docroot/CRI/content/CR_2_2_1X_How_many_women_get_ovarian_cancer_33.asp?sitearea=.
2. Aggarwal BB, Kumar A, Bharti AC. Anticancer potential of curcumin: preclinical and clinical studies. Anticancer Res 2003;23:363–98.
3. Sharma RA, Gescher AJ, Steward WP. Curcumin: the story so far. Eur J Cancer 2005;41:1955–68.
4. Holt PR, Katz S, Kirshoff R. Curcumin therapy in inflammatory bowel disease: a pilot study. Dig Dis Sci 2005;50:2191–3.
5. Aggarwal S, Ichikawa H, Takada Y, Sandur SK, Shishodia S, Aggarwal BB. Curcumin (diferuloylmethane) down-regulates expression of cell proliferation and antiapoptotic and metastatic gene products through suppression of IκBα kinase and Akt activation. Mol Pharmacol 2006;69:195–206.
6. Bharti AC, Donato N, Aggarwal BB. Curcumin (diferuloylmethane) inhibits constitutive and IL-6-inducible STAT3 phosphorylation in human multiple myeloma cells. J Immunol 2003;171:3863–71.
7. Kawamori T, Lubet R, Steele VE, et al. Chemopreventive effect of curcumin, a naturally occurring anti-inflammatory agent, during the promotion/progression stages of colon cancer. Cancer Res 1999;59:597–601.
8. Aggarwal BB, Shishodia S, Takada Y, et al. Curcumin suppresses the paclitaxel-induced nuclear factor-κB pathway in breast cancer cells and inhibits lung metastasis of human breast cancer in nude mice. Clin Cancer Res 2005;11:7490–8.
9. Cruz-Correa M, Shoskes DA, Sanchez P, et al. Combination treatment with curcumin and quercetin of adenomas in familial adenomatous polyposis. Clin Gastroenterol Hepatol 2006;4:1035–8.
10. LoTempio MM, Veena MS, Steele HL, et al. Curcumin suppresses growth of head and neck squamous cell carcinoma. Clin Cancer Res 2005;11:6994–7002.
11. Yu YY, Li Q, Zhu ZG. NF-κB as a molecular target in adjuvant therapy of gastrointestinal carcinomas. Eur J Surg Oncol 2005;31:386–92.
12. Yan C, Jamaluddin MS, Aggarwal B, Myers J, Boyd DD. Gene expression profiling identifies activating transcription factor 3 as a novel contributor to the proapoptotic effect of curcumin. Mol Cancer Ther 2005;4:233–41.
13. Li L, Braiteh FS, Kurzrock R. Liposome-encapsulated curcumin: *in vitro* and *in vivo* effects on proliferation, apoptosis, signaling, and angiogenesis. Cancer 2005;104:1322–31.
14. Aggarwal BB. Nuclear factor-κB: the enemy within. Cancer Cell 2004;6:203–8.
15. Dobrovolskaia MA, Kozlov SV. Inflammation and cancer: when NF-κB amalgamates the perilous partnership. Curr Cancer Drug Targets 2005;5:325–44.
16. Kang G, Kong PJ, Yuh YJ, et al. Curcumin suppresses lipopolysaccharide-induced cyclooxygenase-2 expression by inhibiting activator protein 1 and nuclear factor κb bindings in BV2 microglial cells. J Pharmacol Sci 2004;94:325–8.
17. Karin M, Cao Y, Greten FR, Li ZW. NF-κB in cancer: from innocent bystander to major culprit. Nat Rev Cancer 2002;2:301–10.
18. Yamamoto Y, Gaynor RB. Role of the NF-κB pathway in the pathogenesis of human disease states. Curr Mol Med 2001;1:287–96.
19. Takada Y, Kobayashi Y, Aggarwal BB. Evodiamine abolishes constitutive and inducible NF-κB activation by inhibiting IκBα kinase activation, thereby suppressing NF-κB-regulated antiapoptotic and metastatic gene expression, up-regulating apoptosis, and inhibiting invasion. J Biol Chem 2005;280:17203–12.
20. Aghajanian C, Dizon DS, Sabbatini P, Raizer JJ, Dupont J, Spriggs DR. Phase I trial of bortezomib and carboplatin in recurrent ovarian or primary peritoneal cancer. J Clin Oncol 2005;23:5943–9.
21. Yu D, Wolf JK, Scanlon M, Price JE, Hung MC. Enhanced c-erbB-2/neu expression in human ovarian cancer cells correlates with more severe malignancy that can be suppressed by E1A. Cancer Res 1993;53:891–8.
22. Buick RN, Pullano R, Trent JM. Comparative properties of five human ovarian adenocarcinoma cell lines. Cancer Res 1985;45:3668–76.
23. Yoneda J, Kuniyasu H, Crispens MA, Price JE, Bucana CD, Fidler IJ. Expression of angiogenesis-related genes and progression of human ovarian carcinomas in nude mice. J Natl Cancer Inst 1998;90:447–54.
24. Shishodia S, Majumdar S, Banerjee S, Aggarwal BB. Ursolic acid inhibits nuclear factor-κB activation induced by carcinogenic agents through suppression of IκBα kinase and p65 phosphorylation: correlation with down-regulation of cyclooxygenase 2, matrix metalloproteinase 9, and cyclin D1. Cancer Res 2003;63:4375–83.
25. Takada Y, Singh S, Aggarwal BB. Identification of a p65 peptide that selectively inhibits NF-κB activation induced by various inflammatory stimuli and its role in down-regulation of NF-κB-mediated gene expression and up-regulation of apoptosis. J Biol Chem 2004;279:15096–104.
26. Takada Y, Khuri FR, Aggarwal BB. Protein farnesyltransferase inhibitor (SCH 66336) abolishes NF-κB activation induced by various carcinogens and inflammatory stimuli leading to suppression of NF-κB-regulated gene expression and up-regulation of apoptosis. J Biol Chem 2004;279:26287–99.
27. Han LY, Landen CN, Trevino JG, et al. Antiangiogenic and antitumor effects of SRC inhibition in ovarian carcinoma. Cancer Res 2006;66:8633–9.
28. Landen CN, Jr., Chavez-Reyes A, Bucana C, et al. Therapeutic EphA2 gene targeting *in vivo* using neutral liposomal small interfering RNA delivery. Cancer Res 2005;65:6910–8.
29. Landen CN, Jr., Lu C, Han LY, et al. Efficacy and antivascular effects of EphA2 reduction with an agonistic antibody in ovarian cancer. J Natl Cancer Inst 2006;98:1558–70.
30. Halder J, Kamat AA, Landen CN, Jr., et al. Focal adhesion kinase targeting using *in vivo* short interfering RNA delivery in neutral liposomes for ovarian carcinoma therapy. Clin Cancer Res 2006;12:4916–24.
31. Thaker PH, Han LY, Kamat AA, et al. Chronic stress promotes tumor growth and angiogenesis in a mouse model of ovarian carcinoma. Nat Med 2006;12:939–44.
32. Hsu Y, Sood AK, Sorosky JI. Docetaxel versus paclitaxel for adjuvant treatment of ovarian cancer: case-control analysis of toxicity. Am J Clin Oncol 2004;27:14–8.
33. Vasey PA, Jayson GC, Gordon A, et al. Phase III randomized trial of docetaxel-carboplatin versus paclitaxel-carboplatin as first-line chemotherapy for ovarian carcinoma. J Natl Cancer Inst 2004;96:1682–91.
34. Kamat AA, Kim TJ, Landen CN, Jr., et al. Metronomic chemotherapy enhances the efficacy of antivascular therapy in ovarian cancer. Cancer Res 2007;67:281–8.
35. Huang S, DeGuzman A, Bucana CD, Fidler IJ. Nuclear factor-κB activity correlates with growth, angiogenesis, and metastasis of human melanoma cells in nude mice. Clin Cancer Res 2000;6:2573–81.
36. Yamamoto Y, Gaynor RB. Therapeutic potential of inhibition of the NF-κB pathway in the treatment of inflammation and cancer. J Clin Invest 2001;107:135–42.
37. Shi M, Cai Q, Yao L, Mao Y, Ming Y, Ouyang G. Antiproliferation and apoptosis induced by curcumin in human ovarian cancer cells. Cell Biol Int 2006;30:221–6.
38. Wallace JM. Nutritional and botanical modulation of the inflammatory cascade—eicosanoids, cyclooxygenases, and lipoxygenases—as an adjunct in cancer therapy. Integr Cancer Ther 2002;1:7–37;discussion.
39. Siwak DR, Shishodia S, Aggarwal BB, Kurzrock R. Curcumin-induced antiproliferative and proapoptotic effects in melanoma cells are associated with suppression of IκB kinase and nuclear factor κB activity and are independent of the B-Raf/mitogen-activated/extracellular signal-regulated protein kinase pathway and the Akt pathway. Cancer 2005;104:879–90.
40. Ghosh S, Karin M. Missing pieces in the NF-κB puzzle. Cell 2002;109 Suppl:S81–96.
41. Lev-Ari S, Zinger H, Kazanov D, et al. Curcumin synergistically potentiates the growth inhibitory and pro-apoptotic effects of celecoxib in pancreatic adenocarcinoma cells. Biomed Pharmacother 2005;59 Suppl 2:S276–80.
42. Lev-Ari S, Strier L, Kazanov D, et al. Celecoxib and curcumin synergistically inhibit the growth of colorectal cancer cells. Clin Cancer Res 2005;11:6738–44.
43. Satoskar RR, Shah SJ, Shenoy SG. Evaluation of anti-inflammatory property of curcumin (diferuloyl methane) in patients with postoperative inflammation. Int J Clin Pharmacol Ther Toxicol 1986;24:651–4.
44. Deodhar SD, Sethi R, Srimal RC. Preliminary study on antirheumatic activity of curcumin (diferuloyl methane). Indian J Med Res 1980;71:632–4.
45. Cheng AL, Hsu CH, Lin JK, et al. Phase I clinical trial of curcumin, a chemopreventive agent, in patients with high-risk or pre-malignant lesions. Anticancer Res 2001;21:2895–900.
46. Lao CD, Ruffin MTt, Normolle D, et al. Dose escalation of a curcuminoid formulation. BMC Complement Altern Med 2006;6:10.
47. Shoba G, Joy D, Joseph T, Majeed M, Rajendran R, Srinivas PS. Influence of piperine on the pharmacokinetics of curcumin in animals and human volunteers. Planta Med 1998;64:353–6.
48. Sharma RA, McLelland HR, Hill KA, et al. Pharmacodynamic and pharmacokinetic study of oral Curcuma extract in patients with colorectal cancer. Clin Cancer Res 2001;7:1894–900.